HUMAN BiOLOGY AND PUBLiC HEALTH JOURNAL OF THE AUXOLOGICAL SOCIETY

ISSN 2748-9957 | Vol. 3 2021 | pp. 1–23

Network reconstruction based on synthetic data generated by a Monte Carlo approach

Masiar Novine[1] • Cecilie Cordua Mattsson[2] • Detlef Groth[1]

[1] University of Potsdam, Institute of Biochemistry and Biology, Bioinformatics Group, 14469 Potsdam, Germany.
[2] ADBOU, Institute of Forensic Medicine, University of Southern Denmark, Campusvej 55, DK 5230 Odense M, Denmark.

Citation:

Novine, M./Mattsson, C./Groth, D. (2021). Network reconstruction based on synthetic data generated by a Monte Carlo approach, Human Biology and Public Health 3.
https://doi.org/10.52905/hbph2021.3.26.

Received: 2021-11-02
Accepted: 2022-03-31
Published: 2022-06-16

Conflict of Interest:

There are no conflicts of interest.

Correspondence to:

Masiar Novine
email: novinefarahb@uni-potsdam.de

Keywords:

Monte Carlo method, network science, network reconstruction, mcgraph, random sampling, linear enamel hypoplasia

Abstract

Background Network models are useful tools for researchers to simplify and understand investigated systems. Yet, the assessment of methods for network construction is often uncertain. Random resampling simulations can aid to assess methods, provided synthetic data exists for reliable network construction.

Objectives We implemented a new Monte Carlo algorithm to create simulated data for network reconstruction, tested the influence of adjusted parameters and used simulations to select a method for network model estimation based on real-world data. We hypothesized, that reconstructs based on Monte Carlo data are scored at least as good compared to a benchmark.

Methods Simulated data was generated in R using the Monte Carlo algorithm of the *mcgraph* package. Benchmark data was created by the *huge* package. Networks were reconstructed using six estimator functions and scored by four classification metrics. For compatibility tests of mean score differences, Welch's *t*-test was used. Network model estimation based on real-world data was done by stepwise selection.

Samples Simulated data was generated based on 640 input graphs of various types and sizes. The real-world dataset consisted of 67 medieval skeletons of females and males from the region of Refshale (Lolland) and Nordby (Jutland) in Denmark.

Results Results after *t*-tests and determining confidence intervals (CI95%) show, that evaluation scores for network reconstructs based on the *mcgraph* package were at least as good compared to the benchmark *huge*. The results even indicate slightly better scores on average for the *mcgraph* package.

Conclusion The results confirmed our objective and suggested that Monte Carlo data can keep up with the benchmark in the applied test framework. The algorithm offers the feature to use (weighted) un- and directed graphs and might be useful for assessing methods for network construction.

Take home message for students Random sampling is a simple, but effective approach. It can be used in the context of network analysis to access the quality of network reconstruction methods.

Introduction

Networks are visualized by graphs, where variables are represented as nodes, while associations are depicted as edges (i.e., lines between nodes). Using such a form of representation, graphs can help to simplify a complex system by focusing on the relationships of its members (Barabási and Pósfai 2016) (e.g., see figure 1 for an example, illustrating some advantages of graph models in comparison to alternative ways of visualization). Network analysis uses graph theory to investigate the structure of networks. In the context of social science, social network analysis is used to analyze interactions of social members, called actors (nodes) and focuses on their relationships (edges). Associations can represent communication, exchange of goods or emotional affection in the case of friendship networks (Wasserman and Faust 1994). Next to the static understanding of networks, temporal networks transmit changes of network structures over time. Snapshots of networks at consecutive time points can be analyzed by concepts of temporal correlation or temporal overlap (Nicosia et al. 2013). The first denotes with which probability associations remain over time, while the second addresses the time-dependent similarity of networks. Such approaches can be useful to uncover dynamic systems like modeling trade movements of livestock (Büttner et al. 2016).

In the context of public health, network medicine investigates the interrelationship of hierarchies of multiple networks (i.e., social, disease and metabolic / genetic networks) to uncover phenomena like disease (Barabási et al. 2011; Loscalzo et al. 2017). For example, while there is a genetic influence on obesity (Frayling et al. 2007), the influence of social factors like friendship on the risk of a person becoming obese could be shown to be more important by considering social and underlying genetic networks. Obesity clusters in social communities made of friendship and family networks (Christakis and Fowler 2007; Barabási 2007).

Network construction methods

Constructing network models usually requires information about the relevance of particular associations between certain variables. Selecting the relevant variables thus, is crucial. Stepwise regression (Heinze et al. 2018) based on each node can be used but this approach requires selecting thresholds and by including / removing one variable at a time seriously biases basic statistics of regression analysis, leading to upward biased R^2 values, too low standard errors for regression coefficients, too low p-values and too large absolute values for coefficients (Copas and Long 1991; Harrell 2001). Some of the problems can be solved by using graphical *lasso* for regulating coefficients (Friedman et al. 2008) and stability selection (Meinshausen and Bühlmann 2006; Meinshausen and Bühlmann 2010). Other approaches calculate the correlation matrix based on all variables and apply (hard) correlation thresholds to filter relevant associations (Rice et al. 2005; Batushansky et al. 2016; Sulaimanov and Koeppl 2016) or use power transforms to perform soft thresholding (Zhang and Horvath 2005; Ghazalpour et al. 2006; Langfelder and Horvath 2008). The later approach aims to avoid loss of information by binarization. *St. Nicolas House Analysis* (SNHA) constructs networks based on *association chains of variables* based on their correlations. The method has advantages as it is non-parametric and there is no need to specify a selection threshold for including variables (Groth et al. 2019; Hermanussen et al. 2021).

Using simulated data for assessment of network construction methods

Evaluating the applied method is critical when constructing network models. Estimating the scale of the possible error becomes difficult, because the interactions of variables in a network might be complex. Motivated by the fact, that randomized resampling approaches like bootstrapping are routinely applied for statistical analysis to empirically determine error terms

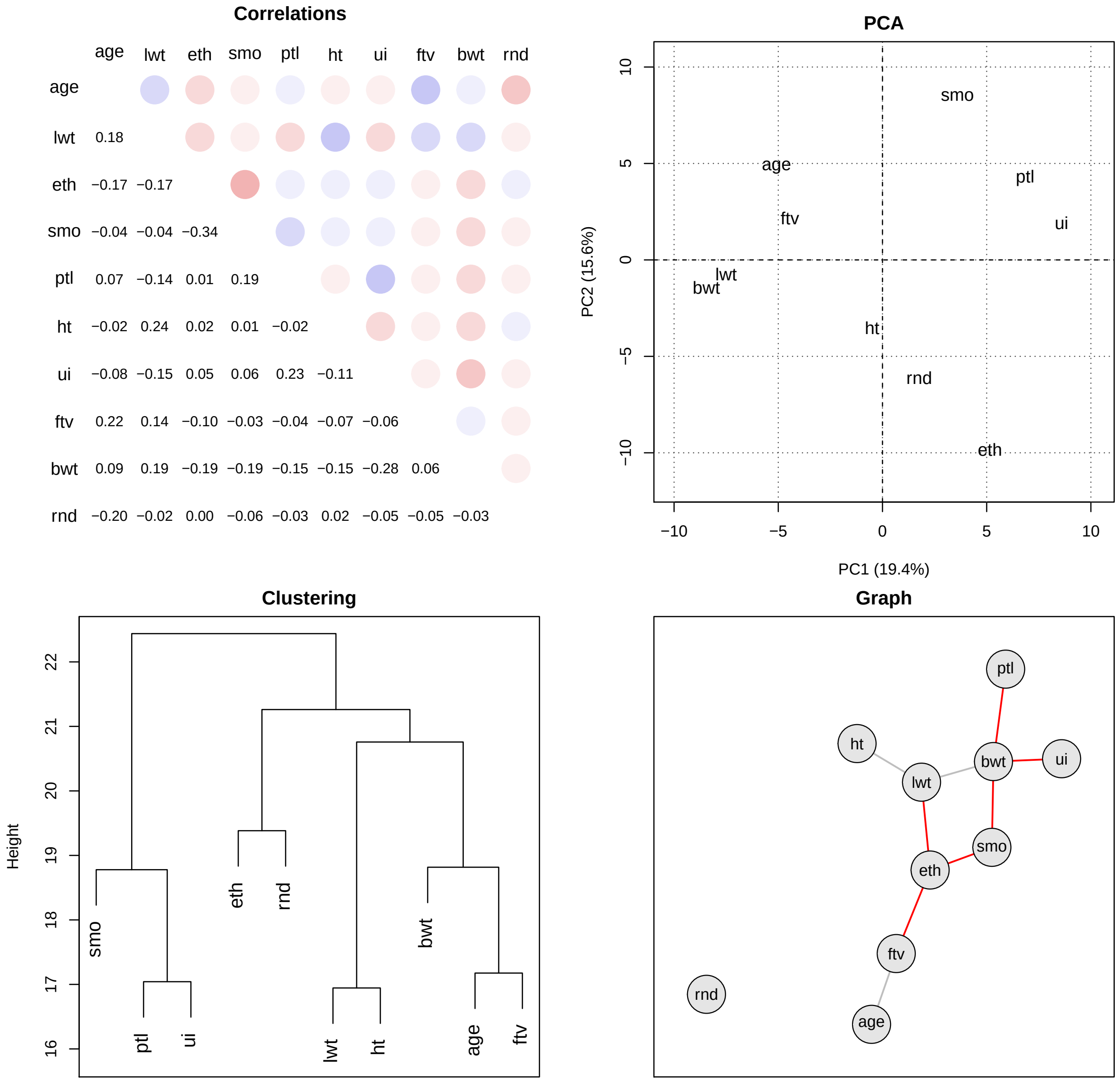

	age	lwt	eth	smo	ptl	ht	ui	ftv	bwt	rnd
age		●	●	●	●	●	●	●	●	●
lwt	0.18		●	●	●	●	●	●	●	●
eth	−0.17	−0.17		●	●	●	●	●	●	●
smo	−0.04	−0.04	−0.34		●	●	●	●	●	●
ptl	0.07	−0.14	0.01	0.19		●	●	●	●	●
ht	−0.02	0.24	0.02	0.01	−0.02		●	●	●	●
ui	−0.08	−0.15	0.05	0.06	0.23	−0.11		●	●	●
ftv	0.22	0.14	−0.10	−0.03	−0.04	−0.07	−0.06		●	●
bwt	0.09	0.19	−0.19	−0.19	−0.15	−0.15	−0.28	0.06		●
rnd	−0.20	−0.02	0.00	−0.06	−0.03	0.02	−0.05	−0.05	−0.03	

Figure 1 Comparison of multivariate data techniques. Next to the correlations, the results of a PCA, a dendrogram based on clustering and a graph are depicted using the same example data set. The set contains data of variables related to the health status of 189 children and their mothers, collected at Baystate Medical Center, Springfield, Mass during 1986: age – mother's age in years, lwt – mother's weight in pounds at last menstrual period, eth – mother's ethnicity (1 = white, 2 = black, 3 = other), smo – smoking status during pregnancy (0 = no, 1 = yes), ptl – number of previous premature labours, ht – history of hypertension (0 = no, 1 = yes), ui – presence of uterine irritability (0 = no, 1 = yes), ftv -number of physician visits during the first trimester, bwt birth weight of child in grams, rnd – some random uncorrelated data. For graph construction the St. Nicolas House algorithm was used (Groth et al. 2019; Hermanussen et al. 2021).

or confidence intervals (Efron and Tibshirani 1986), we think, that a simulation-driven approach could aid assessing a certain network construction method. We use an approach based on the Monte Carlo method (Metropolis and Ulam 1949) due to its simplicity. We describe the approach in the method section in more detail.

Our approach allows for flexible random data generation on pre-defined graph structures, which is superior to most example data provided by statistical software (e.g., R). We want to provide a simple tool to uncover strengths and limitations of methods. In view of the notion, that "the art of data analysis is about choosing and using multiple tools" (Harrell 2001), our approach is embedded in a broader framework of statistical analyses.

Our presented analysis proceeded as follows: We generated synthetic data based on pre-defined network structures of various network types and sizes, performed network reconstruction and finally evaluated the network reconstructs by binary classification. Such a testing framework can identify suitable candidate models or identify weaknesses of modeling approaches by investigating on how precise and sensitive predictions of associations between the variables are.

We tested the hypothesis, that network reconstructs based on the Monte Carlo approach are scored at least as good compared to a benchmark. For comparison, we used the data generation function of the R package *huge*. We also altered parameters of the Monte Carlo function to assess their influence on scores of network reconstructs. Finally, we applied a well-scored network construction method to construct a network model based on real-world data (Mattsson 2021).

Samples and methods

Software

For most of the computations and programming we used the programming language R (R Core Team 2021) version 4.0.4. Time critical parts were implemented in C++ via the interfaces *Rcpp* (Eddelbuettel and François 2011) version 1.0.7 and *RcppArmadillo* (Eddelbuettel and Sanderson 2014) version 0.10.7.0.0, enabling access to the C++ library Armadillo (Sanderson and Curtin 2016), (Sanderson and Curtin 2018) version 10.6. Embedding data into the manuscript and formatting of tables was done by dynamic report generation using *knitr* (Xie 2021) version 1.36 and *xtable* (Dahl et al. 2000) version 1.8-4. We used our R package *mcgraph* (Groth and Novine 2022) version 0.5.0 for most of the computational work, including synthetic data generation, data imputation, creation of network structures, estimation of networks, evaluation of estimates and graph visualization. As a benchmark for the Monte Carlo data, the *huge* package (Zhao et al. 2012) version 1.3.5 was used. Statistical analysis and graphics were done using R standard packages and *ggplot2* (Wickham 2016) version 3.3.5.

Classification metrics for assessment of network reconstructs

We reframed the task of network reconstruction as a binary classification problem. Based on raw data, an estimator function (i.e., a classifier) was applied to classify edges as being present (positive case) or absent (negative case). By comparing the classification results to the true network structure, the classification can be evaluated.

We briefly defined the possible outcomes of the classification:

- true-positive (TP): correct classification of an edge as being present
- true-negative (TN): correct classification of an edge as being absent
- false-positive (FP): incorrect classification of an edge as being present
- false-negative (FN): incorrect classification of an edge as being absent

For evaluation we used four metrics (see Table 1 for a detailed list):

1. AUC, Area Under the Receiver Operating Characteristic (ROC) curve (Hanley and McNeil 1982), sensitivity (TPR) plotted against FPR.
2. PR-AUC, area under the Precision-Recall Curve (PRC), precision (PPV) plotted against sensitivity (TPR).
3. averaged Balanced Classification Rate (BCR)
4. averaged and normalized variant of Matthews Correlation Coefficient (norm-MCC) (Matthews 1975)

Each classification metric is based on another scoring scheme, so that classification results should eventually be different. In general, for metrics in the range of 0 to 1, values of 0.5 indicate classification results not better than random. In ROC and PRC plots, this is indicated by the baseline diagonal. Mostly, networks are sparse, so that the set of underlying classes is imbalanced (i.e., the number of absent edges is much higher than that of present ones). In such cases PR-AUC is preferred over AUC, because PRC plots capture the relationship

Table 1 Summary of metrics used for the evaluation of classification results. The formula for the calculation of the Area Under the ROC curve and PRC is based on the trapezoid rule. The variable r denotes the number of classification results, including those points located at (0, 0) and (1, 1) in the ROC curve plot, which are set as start and end values. For the Precision-Recall Curve (PRC) those coordinates are switched. For MCC a normalized version based on (Cao et al. 2020) is given, scaling it to the range of 0 to 1. Next to the formula for the calculation, the best and the worst possible scores for each metric are included.

Metric	Abbreviation	Calculation	Worst	Best
Sensitivity	TPR	$\frac{TP}{(TP+FN)}$	0	1
Specificity	TNR	$\frac{TN}{(TN+FP)}$	0	1
Precision	PPV	$\frac{TP}{(TP+FP)}$	0	1
False-Positive Rate	FPR	$\frac{FP}{FP+TN} = 1 - TNR$	1	0
Area Under the ROC curve	AUC	$\sum_{i=1}^{r-1} \frac{(TPR_i+TPR_{i+1})(FPR_{i+1}-FPR_i)}{2}$	0	1
Area Under the PRC	PR-AUC	$\sum_{i=1}^{r-1} \frac{(PPV_i+PPV_{i+1})(TPR_{i+1}- TPR_i)}{2}$	0	1
Balanced Classification Rate	BCR	$\frac{(TPR+TNR)}{2}$	0	1
Matthews Correlation Coefficient	MCC	$\frac{(TP \cdot TN - FP \cdot FN)}{\sqrt{(TP+FP)(TP+FN)(TN+FP)(TN+FN)}}$	-1	1
Normalized Matthews Correlation Coefficient	norm-MCC	$\frac{(MCC+1)}{2}$	0	1

between PPV and TPR, both concerned with the fraction of TP among prediction outcomes. AUC on the other hand relies on FPR, which has the number of TN cases in the denominator. This number will be overwhelmingly higher in the case of sparse networks and will push the value of FPR towards 0 (i.e., best score) leading to an overly optimistic and misleading AUC (Cao et al. 2020; Chicco and Jurman 2020). Next to AUC and PR-AUC, we additionally used BCR and norm-MCC to (1) express the underlying characteristics of the data better (2) illustrate and control for differences of the scoring values and (3) compare trends across metrics.

Proposed Monte Carlo method for simulated data generation

Input graphs

The input for the data generation algorithm is either an (weighted) un- or directed graph. Assume an initial graph G with a set of nodes $V(G)$ with $V = \{1, 2, \ldots, p\}$ and a set of edges $E(G)$ with $E \subseteq V \times V$. Computationally, we represent the graph in form of an adjacency matrix (i.e., a binary square matrix with the dimensions $p \times p$, with p being the number of nodes given by the size of the set $V(G)$). We denote $E \subseteq \{(u, v) \mid u, v \in V, u \neq v\}$, such that $e(u, v) : = (e_{uv}|e_{uv} \neq e_{vu})$ is a directed edge between node u and v. Consequently, an undirected edge is given as $e(u, v) : = (e_{uv}|e_{uv} = e_{vu})$. We define a weight function $w: E \rightarrow \mathbb{R}$, such that $w(e_{uv})$ is a weighted edge. We call an edge between u and v simple, if $|w(e_{uv})| = 1$. Throughout our analysis, we only considered simple edges. Edges are indicated by non-zero entries in the according field of the matrix. Positive or negative edges indicate positive or negative associations between the according variables, respectively. A directed graph is represented by a non-symmetric adjacency matrix, while the adjacency matrix of an undirected graph is symmetric (i.e., dividing the matrix along the diagonal leads to the two halves behaving as image and reflection). Finally, we defined the relationship of two connected nodes as follows: A source node is a node, where the edge originates from, and the target node is a node where the according edge ends in. Sometimes we call the source *incoming neighbor* and the target *outgoing neighbor*.

Listing 1 Pseudocode for the Monte Carlo data generation algorithm

```
Input: $p \times p$ adjacency matrix $G$
Output: $p \times n$ matrix $dataMatrix$

procedure monteCarlo($G$, $n$, $iter$, $noise$, $prop$)
    Create empty $p \times n$ $dataMatrix$, where:
    $p$ ← number of nodes
    $n$ ← number of samples per node
    for $i \leftarrow 1$ to $n$ do
        $X_i$ ← Vector with data randomly drawn from $N(\overline{x}, s)$
        for $j \leftarrow 1$ to $iter$ do
            foreach $source$ in shuffle($V(G)$) do
                foreach $target$ in shuffle(neighbors($source$)) do
                    $weight$ ← $w(e_{src,\ trg})$
                    $prop$ ← Proportion source value for updated target value
                    $x'$ ← weightedMean($X_i(source)$, $X_i(target)$, $weight$, $prop$)
                    if $(w(e_{src,\ trg}) < 0)$ then
                        $X_i(target) \leftarrow 2X_i\,(target) - x'$
                    else
                        $X_i(target) \leftarrow x'$
                endfor
            endfor
            Add $noise$ to values
        endfor
        Assign values of $X_i$ to the $i$-th column of $dataMatrix$
    endfor
    return $dataMatrix$
```

Steps of Monte Carlo sampling

Monte Carlo sampling is done based on the following iterative approach:

1. p data values are randomly chosen from a normal distribution with a given mean $\overline{x}$ and a given standard deviation s based on the probability density function
2. $N(\overline{x}, s) = \frac{1}{s\sqrt{2\pi}} exp\left(-\frac{1}{2s^2}\left(x - \overline{x}\right)^2\right), x \in \mathbb{R}$
3. and assigned to each node in the set $V(G)$.
4. A source node is randomly chosen from the set $V(G)$ without replacement and all its outgoing neighbors are found.
5. From the set of outgoing neighbors, a target node is randomly chosen and the weighted mean between source and target is calculated based on
6. $x' = x_{src} \cdot prop \cdot |w(e_{src,trg})| + x_{\mathrm{trg}} \cdot (1 - prop) \cdot |w(e_{src,trg})|$
7. The initial value of the target is then replaced by the newly calculated value. By adjusting a proportion argument ($prop$) the user can determine, how the mean is weighted (e.g., setting $prop = 0.1$ would indicate, that the updated value for the target node is calculated by taking 90% of its prior value and 10% of the value of the source node and then multiplying the proportion with the absolute values of the respective edge weights). Hence, over time the value for the target becomes more correlated to the value of the source.
8. For a given number of iterations, steps 2 and 3 are repeated for all the nodes in $V(G)$ and the total number of outgoing neighbors of each chosen source node, respectively. All the steps are repeated n times, where n corresponds to the number of data values for each node. In the end, the result of the procedure is an

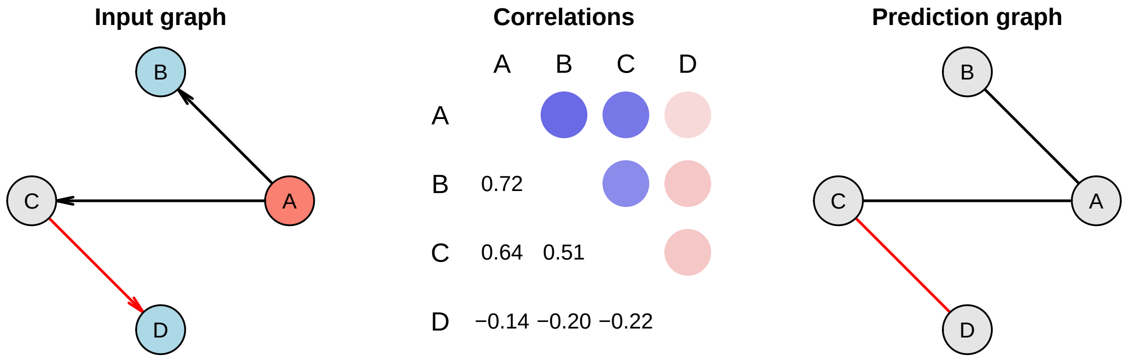

Figure 2 Graphs and data generation. An input graph with its resulting correlation matrix of synthetic data generated for a small network. The input graph with 4 nodes and 3 directed edges (left), the correlation matrix (center) based on synthetic data generated for this small network and a predicted undirected graph based on the underlying data (right). A is a confounder and has a strong positive correlation to B and C. Due to the negative correlation between C and D, both, A and B are also negatively correlated to D, illustrating the influence of indirect associations on the pair-wise correlation of two nodes. The data was generated by the here presented algorithm using the Monte Carlo method. Red edges indicate negative correlations. In the correlation matrix, positive correlations are indicated with a blue circle, while negative correlations are shown as a red circle. The strength of the correlation is depicted by the strength of the color.

$p \times n$ data matrix. In listing 1 the pseudocode of the approach is given.

9. When calculating the weighted mean, the absolute edge weight is also considered, which will influence the mean calculation. If edge weights are negative, first the weighted mean is calculated as previously, but subtracted from twice the value of the target node to get its updated value, making them anti-correlated. It is important to note, that the algorithm defines a source-to-target relationship for each pair of connected nodes, independent of the input graph being directed or not.

Monte Carlo algorithm – How synthetic data is created

The implementation of the algorithm offers several arguments for which input values can be varied to change the shape of the synthetic data (see Table 2 Appendix).

We used the example in figure 2 to illustrate the mechanics of data creation. We assumed simple edges and a value for the influence of the source node on the target ($prop = 0.1$, 10%). For details of the algorithm see Listing 1. The algorithm creates a vector with n random values from $N(100, 2)$ for each variable. In the depicted directed graph, A (source) influences B (target) positively indicated by a directed edge from A to B. For simplicity, let us only consider the first element of the vectors of A and B given for example as $A_1 = 102$ and $B_1 = 104$. Based on the updating rule the new value B_1' is the weighted mean between the two values, so that $B_1' = (102 \cdot 0.1 \cdot |1|) + (104 \cdot (1 - 0.1) \cdot |1|) = 103.8$. Consequently, after multiple iterations the vectors of A and B become similar and are positively correlated. The algorithm adds noise after each iteration to avoid that correlations develop too quickly. Take the case, where C only influences D negatively without any other influence

present (i.e., for the moment we neglect that A influences C positively). Assume $C_1 = 98$ and $D_1 = 100$. In the first step, we calculated the weighted mean between the two values, so that $D_1^* = 99.8$. In the second step we subtracted this result from twice the value of D_1 to get to its updated value, so that $D_1^{'} = (2 \cdot 100 - 99.8) = 100.2$. Hence, C and D become more anti-correlated over time.
Note, that the example network in figure 2 is more complex: A is a confounding variable. It positively influences both B and C. In consequence, B and C become correlated due to their shared association with A. Additionally, this confounding effect leads to an anti-correlation between A, B and D due to the shared association with C (see the correlation matrix in figure 2).

Methods used for network reconstruction

We used following functions for network (re)construction from the *mcgraph* package:
mcg.ct: Simple (hard) correlation thresholding with hard based on a threshold τ to prune the correlated data values and to encode the correlation matrix into a binary adjacency matrix.
mcg.lvs: Stepwise regression (i.e., forward variable selection). One variable after the other was used as a response variable and we preselected the k highest correlated variables of each response as candidates using Pearson correlation. The selection was based on minimizing AIC and at the same time maximizing R^2, while the change in R^2 has to be equal or larger than a given threshold.
mcg.rpart: Forward variable selection using regression trees (Breiman et al. 1984). We again only used the k highest correlated variables for each response variable using Spearman correlation.
Additionally, we used following implementations of the *huge* package:
huge.ct: correlation thresholding
huge.glasso: graphical *lasso* (Friedman et al. 2008)
huge.mb: stability selection (Meinshausen and Bühlmann 2006)

Analysis of parameters of the Monte Carlo algorithm

Based on a cluster network (80 nodes, 235 edges, 3 components) shown in figure 4 we tested the *n*, *iter*, *prop* and *noise* (see Table 2 Appendix) arguments to investigate their influence on PR-AUC scores of network reconstructs. In our simulation test, PR-AUC scores for reconstructs of the cluster network were among the worst, even by methods for which scores has been higher on average. Hence, the network was selected as a suitable candidate for optimization tests. For network reconstruction we used forward variable selection and evaluate the reconstructs. We chose settings for the parameters based on a reasonable range and plot PRCs to illustrate the influence on the reconstructs.

Comparative analysis of Monte Carlo data using network reconstruction

Based on the network types random, scale-free, hub, and cluster (exemplified in figure 3) network reconstruction was done. We used undirected graphs with simple edges. In a first step, the given networks were generated by the *huge.generator* function using the specified graph sizes (20, 40, 80, 400) shown in figure 5. We used the default values for parameters of the function with the number of samples per variable set to $n = 200$. The number of edges was internally determined by the function, as

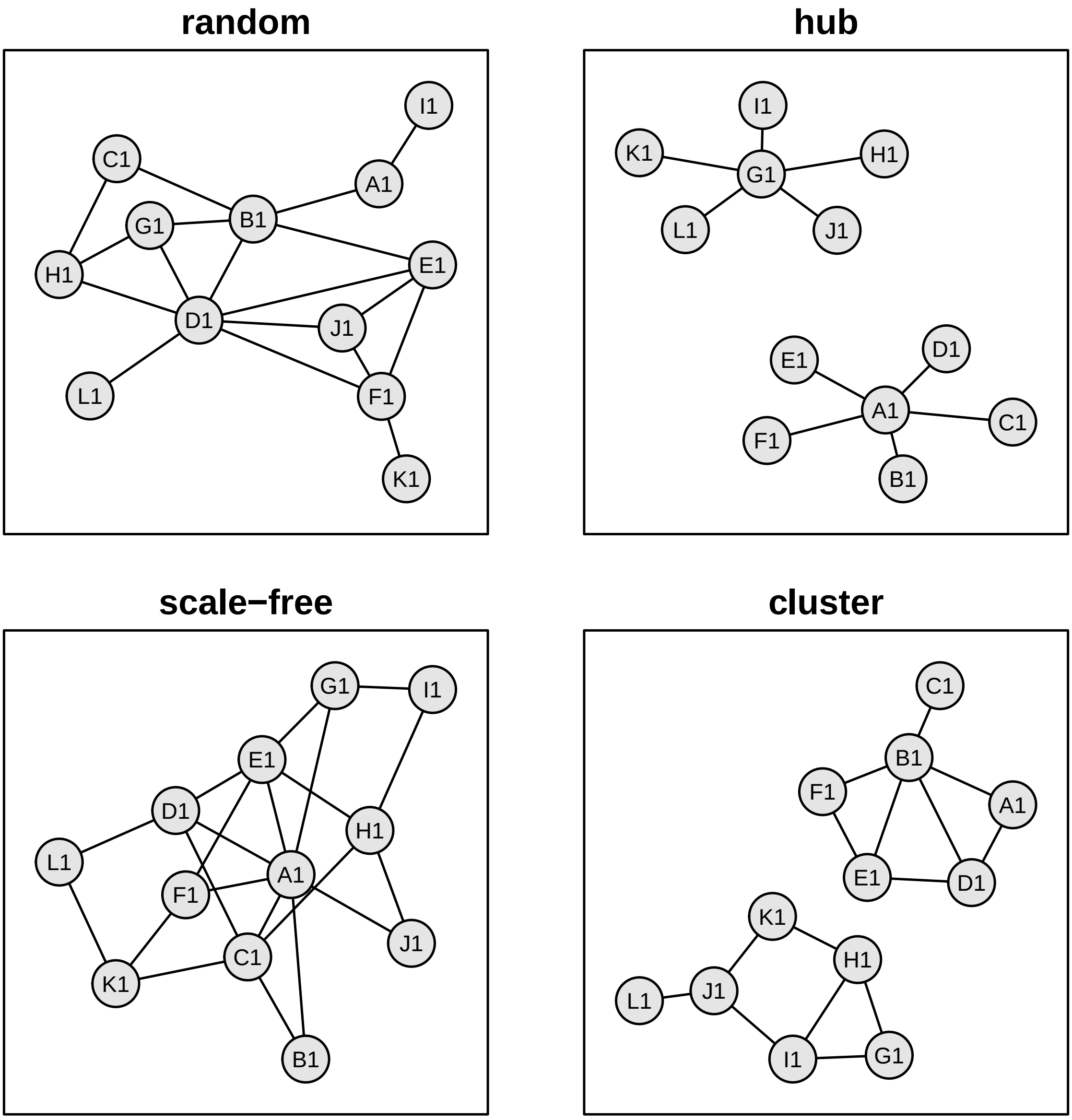

random

hub

scale−free

cluster

Figure 3 Examples of general network types. In our simulation analysis, we used the four network types random, hub, scale-free and cluster to test the influence of the network structure on the quality of reconstructs.

well as the number of components for cluster and hub networks. The generated adjacency matrix was parsed to the *mcgraph* Monte Carlo function *mcg.graph2data* to use the same input graph. The parameters of the function were set to $n = 200$, $iter = 30$, $noise = 1$ and $prop = 0.05$. The classification thresholds, which denote R^2 cutoffs of the *mcgraph* estimators were kept in a reasonable range, spanning from 0 to about 0.1. The values for the tuning parameter λ of the *huge* estimators were automatically calculated as advised by the reference manual (Jiang et al. 2021). Network reconstruction was performed based on the implementations described in the previous section (see *Methods used for network* reconstruction). We evaluated the reconstructs by AUC, PR-AUC, BCR and norm-MCC. To determine significance in mean differences, Welch's t-test was performed as described in literature (Berrar et al. 2007; Wasserman 2013).

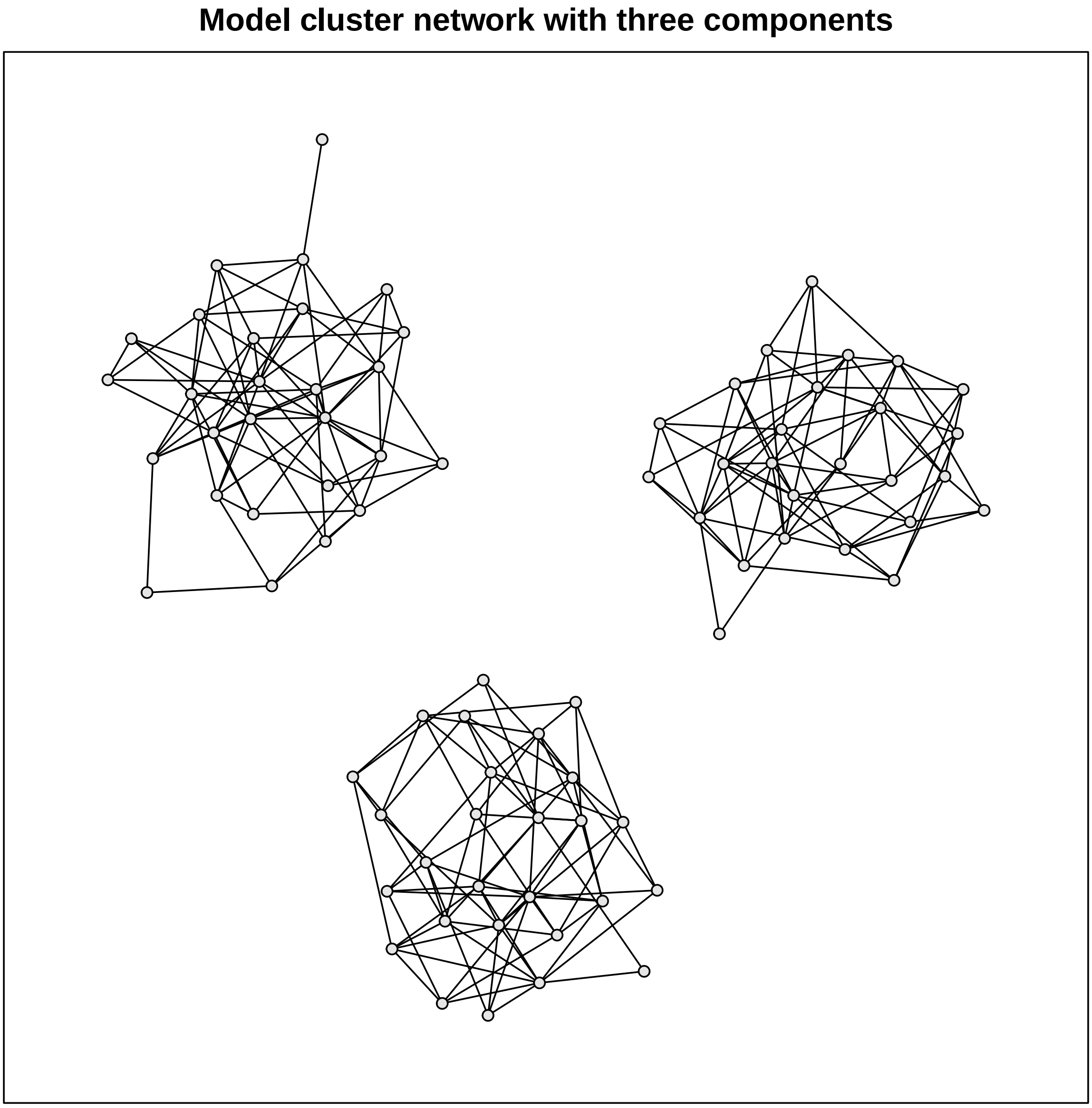

Figure 4 Model cluster network. The depicted cluster network with three components was used as a model network for determining the influence of four key parameters of the Monte Carlo data generation algorithm: iter, prop, noise and the number of samples per variable n.

A real-world example – Analysis of the relationship of linear enamel hypoplasia and bone growth

Sample

We used data from (Mattsson 2021) collected in late 2020 (ADBOU, Unit of Anthropology, Department of Forensic Medicine, University of Southern Denmark). The data set consisted of observations of 67 medieval skeletons of Danish females and males from the region of Refshale (Lolland) and Nordby (Jutland) in Denmark. It included the age of death, which was estimated based on different age markers using a standard method (Milner and Boldsen 2012; Tarp 2017) and the sex of the individuals. Additionally, it contained measurements of the length of the pairs of humeri, radial bones, thigh bones (femora) and shank bones (tibiae). Presence of LEH

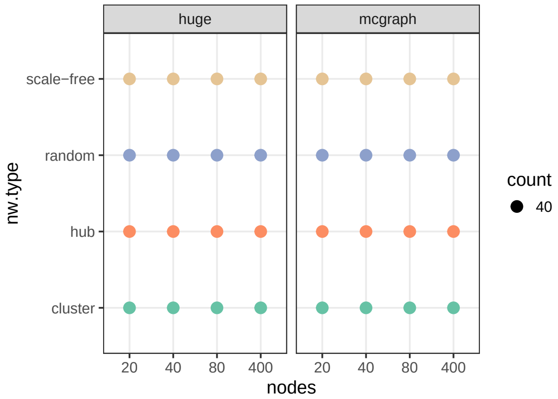

Figure 5 Number of samples for each network type. Regarding both packages, we used random, cluster, hub and scale-free (Barabàsi-Albert) graphs, with number of nodes 20, 40, 80, 400. For each generated graph structure 40 individual graphs were randomly generated, such that the total number of input graphs was 640. After data generation by the huge function (huge.generator), the adjacency matrix of each graph was given to the Monte Carlo data generation function of mcgraph (mcg.graph2data). Subsequently, network reconstruction was performed, followed by evaluation of the reconstructs.

in the canines of both sides of the upper and lower denture was included as a binary assessment.

Sample preparation

Prior to further analysis, we performed data imputation based on regression trees. We calculated the ratio between the lengths of the pairs of humeri and radial bones and the ratio between the lengths of the pairs of thigh bones and shank bones for each sample. Furthermore, we determined the average of the lengths of each bone type.

Network estimation

Our version of stepwise regression was selected based on relatively high scores in our simulation analysis described in the prior section. Using LEH scores of canines of the upper and lower denture, ratios of long bones of arms and legs, lengths of humeri, tibiae, femora, radial and sex, we estimated a network to investigate the relationship between the presence of LEH and the growth of the selected bones. The threshold ΔR^2, which is used for model selection by the stepwise regression algorithm was kept at the default value of 0.04. ΔR^2 denoted the difference of the R^2 values of a model excluding and a model including a candidate variable (i.e., it is the value by which the regression model must improve to justify the inclusion of a variable). We set the number of most correlated candidates per response variable to the default value of $k = 5$. The other selection criterion was a smaller value for Akaikes Information Criterion (AIC) (Akaike 1974; Sakamoto et al. 1986).

Results

The influence of parameters of the Monte Carlo function on the shape of the simulated data was assessed by comparing PR curves of network reconstructs (Figure 6).
A higher number of iterations and a lower value of *prop* improved PR-AUC scores.
The effect of noise on the scores was especially dependent on the number of iterations: While for lower number of iterations (15, 30) the noise level had an impact on scores, such that less noise let to higher scores, this effect disappeared by increasing the number of iterations (60, 120). Higher numbers of samples per variable had the most positive effect on scores: While by using 100 samples per variable, scores were equal to a random classification, the scores improved substantially by using 1000 samples.
We compared scores for network reconstructs based on (1) simulated data of the Monte Carlo approach and based on (2) the data generation function of *huge*. Figure 7 shows box plots on the basis of number of nodes (7A), four selected network types (7B) and six estimator functions (7C)

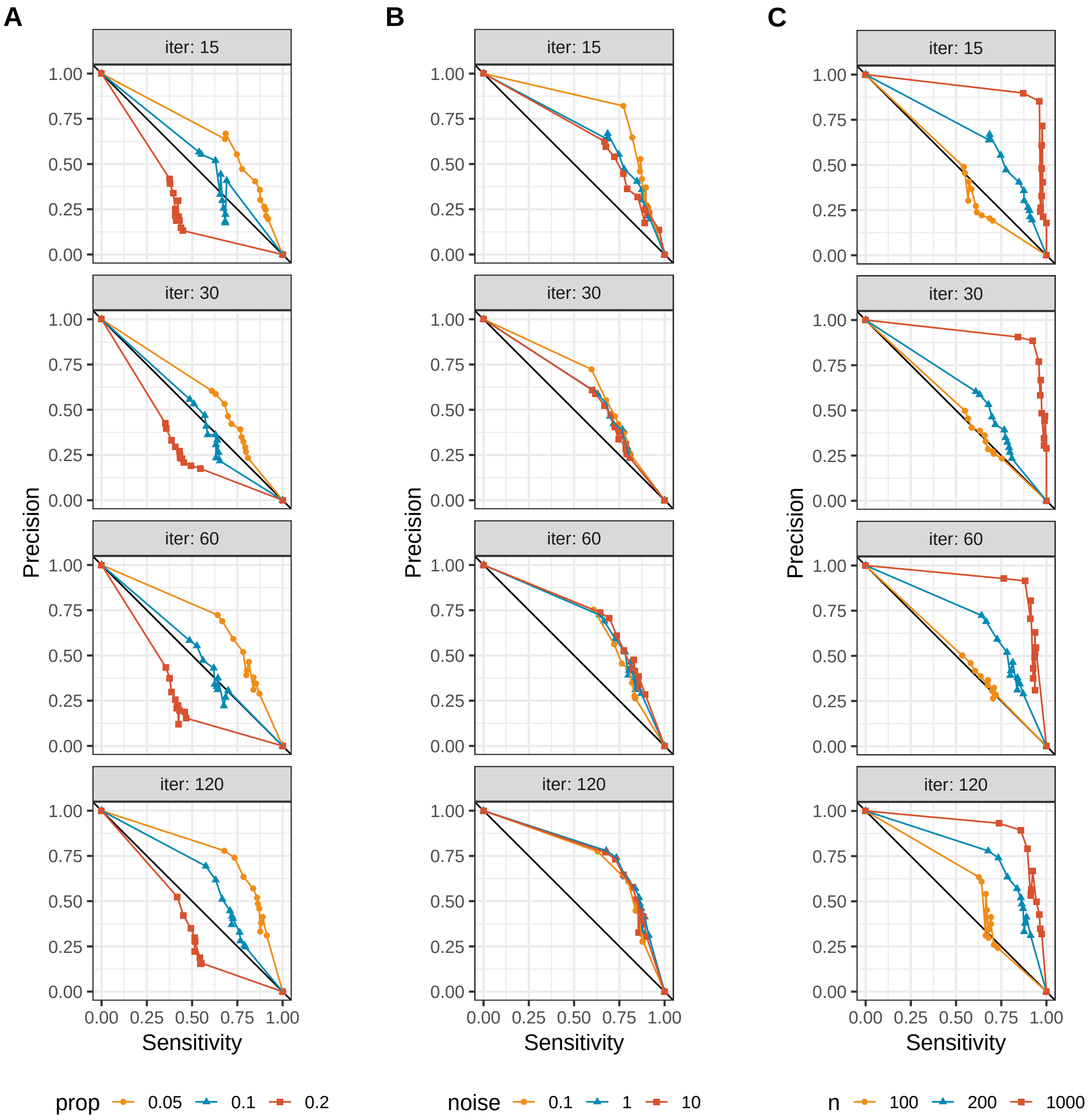

Figure 6 Testing the influence of key parameters of the Monte Carlo data generation function. We performed network reconstruction using stepwise regression based on the cluster network depicted in figure 4. Reconstructs were evaluated by PR-AUC. Four set-ups were tested and in each the number of iterations was doubled (i.e., we used 15, 30, 60 and 120 number of iterations). In (A) we varied the prop argument using the values 5%, 10% and 20%. In (B) the random noise added was 0.1, 1 and 10, respectively. In (C) we varied the values for the number of samples for each variable (100, 200, 1000). The diagonal line is the baseline indicating the result for a random classification.

scored by AUC, PR-AUC, BCR and norm-MCC. Table 3 summarizes the results after applying Welch's *t*-test.

Generally, we observed smaller variability concerning scores for reconstructs based on data of *mcgraph* than for reconstructs based on data of *huge*. This was true across all metrics. Regarding the graph types, except for the hub graph, the median score of reconstructs based on *mcgraph* data was consistently higher. For the rest, there was some variation between metrics. We observed differences between median scores, ranges, skewness of the underlying score distributions and the number of outliers:

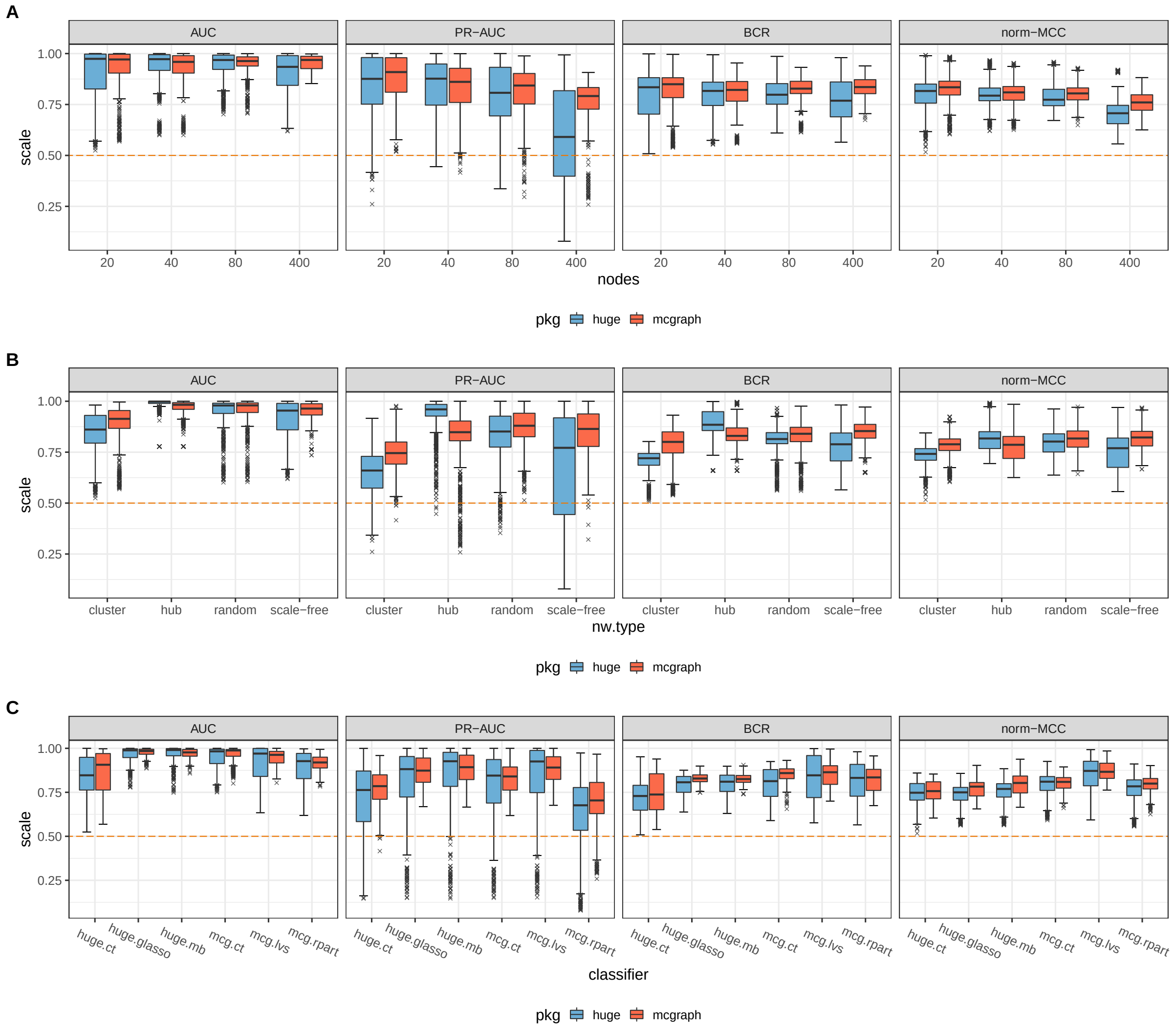

Figure 7 Comparison of prediction quality between huge and mcgraph by number of nodes, network type and classifier. The subplot in (A) shows the results for data generated either by huge or by mcgraph depicted as boxplots for three sets of nodes used for the experiments: 20, 40, 80, 400. The predictions were evaluated by AUC, PR-AUC, BCR and norm-MCC. In (B) the evaluation results are shown based on each network type: cluster, hub, random and scale-free. (C) shows the results for each estimator function: correlation thresholding, glasso, stability selection of huge and correlation thresholding, forward variable selection, variable selection based on decision trees of mcgraph. The orange dashed line indicates a random classification.

- The AUC median score was the highest and the distribution of scores was skewed towards higher values, as indicated by an asymmetry of upper and lower whiskers (i.e., the upper whisker was much smaller than the lower one). In addition, the interquartile ranges (IQRs) had a “squeezed” shape and were mostly located in the upper part of the plot. Most reconstructs were scored best or around one, which indicates low variability. This made comparisons across variables difficult and suggested an overly optimistic evaluation. All AUC scores – including the lower outliers – were located above the baseline level of a random classifier (orange dashed line).
- PR-AUC scores showed the largest IQRs. The median values were lower in comparison to AUC. While there was some tendency of skewness towards higher scores, assessing differences in the upper range was easier

when compared to AUC. Notably, very long IQRs of the scale-free graph type and the largest graph size (400 nodes) were observed for *huge*, while the results of *mcgraph* showed higher median values and smaller IQRs. Some scores had values below the baseline level, implying a more conservative evaluation of reconstructs by PR-AUC compared to AUC, as we would have expected due to the class imbalance.

- The BCR score distribution was less skewed compared to AUC and PR-AUC, as indicated by more equal-sized whiskers. Whiskers and IQRs were generally smaller than for PR-AUC, implying lower variability. The median scores were lower in comparison to AUC and no score fell under the baseline level. Interestingly, while reconstructs of *mcg.rpart* were scored worst by PR-AUC, regarding BCR, they were on a par with the highest scored function mcg.lvs.
- norm-MCC scores resembled scores based on BCR to a large degree: Relatively low variability, with more equal-sized whiskers, some lower and additionally upper outliers regarding the number of nodes and classifier functions, but no score falling below the baseline level.

The results after applying Welch's t-test suggested that mean score differences of zero were probably not compatible with scores across all metrics. Confidence intervals suggested that lower mean values for *huge* compared to *mcgraph* were most likely compatible with resulting scores (see Table 3).

We applied the implementation of stepwise regression (*mcg.lvs*) to estimate a network model for a real-world data set provided by Mattsson. For details see (Mattsson 2021). Figure 8 illustrates the estimated network model. There was no association of scores of LEH in the four canines of upper and lower dentures and the anthropometric measurements of selected bones (humeri, radial bones, thigh bones, shank bones). The LEH binary scores for the canines were present in one component of the cluster graph, while the other component included all variables related to measurements of the selected bones and the sex.

Table 3 Comparison of the overall network reconstruction quality between huge and mcgraph. Network reconstructions were evaluated based on the means of AUC, PR-AUC, BCR and norm-MCC for huge and mcgraph, assumed as class 1 and class 2, respectively. For each metric Welch's t-test ($= 0.05$) was performed. The table shows: mean values for both packages, mean difference $\overline{x}$, standard error SE, upper and lower bounds for the 95% confidence interval of the differences $CI95\%$, t- and p-values, as well as the degrees of freedom df.

	$\overline{x}_{huge}$	$\overline{x}_{mcgraph}$	$\Delta\overline{x}$	SE	$CI95\%_{lb}$	$CI95\%_{ub}$	t-value	p-value	df
AUC	0.923	0.939	-0.016	0.002	-0.020	-0.012	-8.025	0.000	7324.231
PR-AUC	0.774	0.823	-0.049	0.004	-0.056	-0.041	-12.743	0.000	6303.119
BCR	0.795	0.822	-0.028	0.002	-0.032	-0.024	-13.614	0.000	7264.842
norm-MCC	0.775	0.799	-0.024	0.002	-0.027	-0.021	-14.241	0.000	7305.602

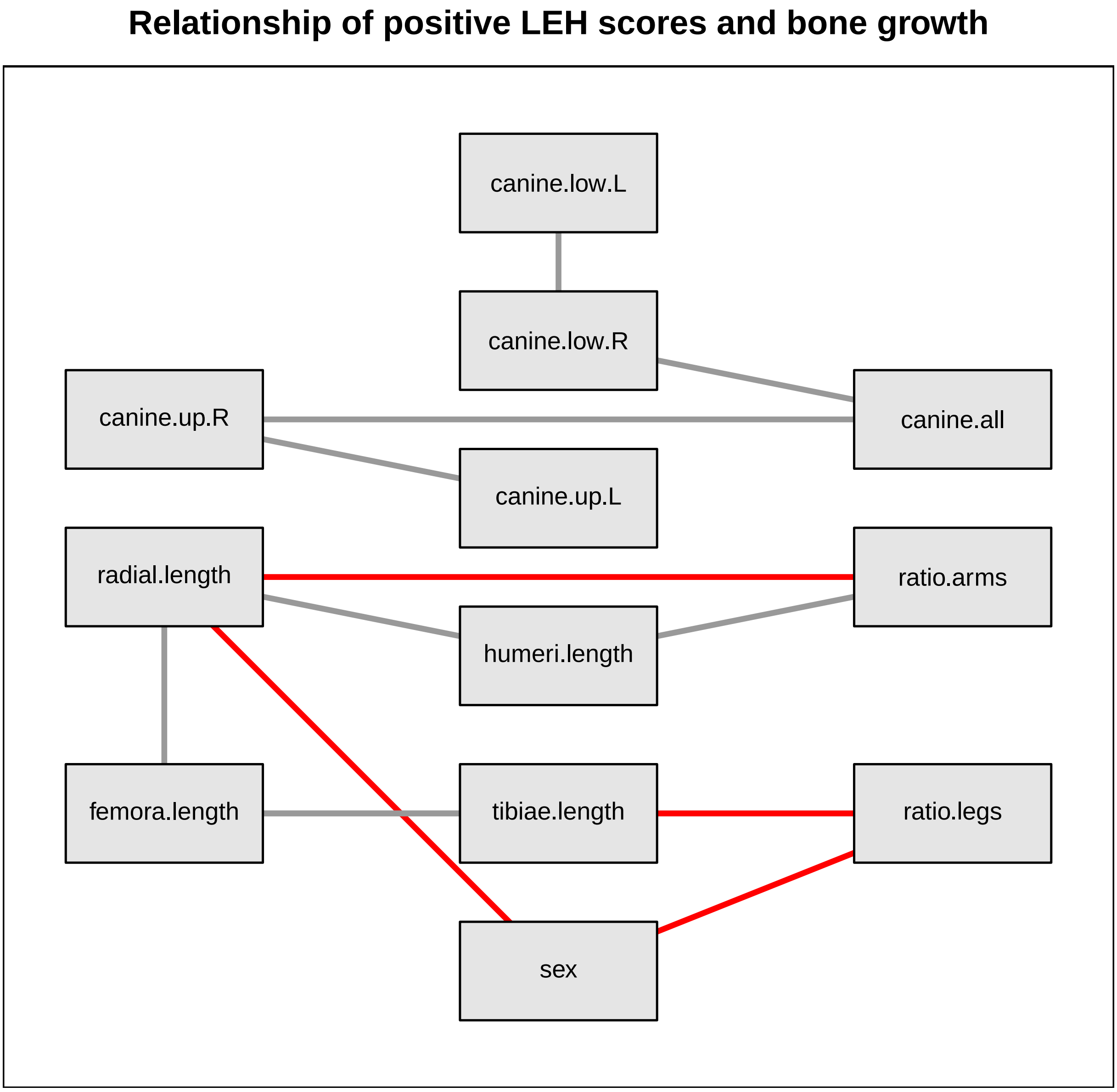

Figure 8 Network model for investigating the association between LEH in canines, bone lengths / ratios and sex. We performed network estimation using stepwise regression ($R^2 = 0.04,\ k = 5$) based on a dataset of 67 medieval skeletons collected from places in Denmark. The four canines of the upper and lower denture were given binary scores indicating the presence of LEH (canine.up.L, canine.up.R, canine.low.L, canine.low.R). Also, the mean for these scores has been calculated (canine.all). For the humeri, radial bones, femora and tibiae the average length was determined (humeri.length, radial.length, femora.length, tibiae.length), next to the ratio between humeri and radial bones (ratio.arms) and the ratio between femora and tibiae (ratio.legs). Additionally, the sex of the individuals is included. According to the network model, there is no association between the LEH scores in canines and the measures of the bones.

Discussion

We applied a simple simulation and testing framework for network reconstruction based on data of a new Monte Carlo algorithm.

We found that network reconstructs can be improved by adjusting key parameters of the function which generates the random data. Increasing the number of samples per variable had the largest influence on the improvement of reconstructs. This is a consequence of general principles of Monte

Carlo sampling (Metropolis and Ulam 1949): When a property like the association between variables is approximated, the accuracy depends on a minimum amount of data coverage. Yet, the main advantage of randomized resampling approaches is that this minimum is often only a small fraction of what would be needed without iterative resampling. In our tests, 1000 samples provided optimal results. Up to date the default sample value for the implementation in *mcgraph* was set to 200, which was a compromise regarding computational cost and the quality of network reconstructs. A smaller value of the proportion argument improved reconstructs. The argument *noise* can be used to distort associations between variables by preventing correlations to develop too quickly. As assumed prior to the test, this effect is counteracted by an increased number of iterations. We set the default value for the number of iterations to 30 to consider quality of reconstructs, but also the runtime of the function. We found good default values of *prop* and *noise* to be 0.05 and 1, respectively. A comprehensive list of arguments, default values and guidelines can be found in Table 1 in *Samples and methods*.

While we concentrated on a cluster network when testing the parameters, we assumed that results for other networks would likely resemble the previously described findings. We did a prescreening using the simulation approach previously described for network structures with various types and sizes. We intentionally used a network, which had scored very poorly. If improvements based on such a poorly rated network are possible, which is the case as we showed, it is likely that these are of general nature. The influence of the parameters can mostly be attributed to the mechanics of the algorithm and the general principles of the Monte Carlo method as a randomized stochastic process (e.g., more samples = better coverage = better approximation).

The comparative analysis of the Monte Carlo simulated data showed higher mean scores for reconstructs based on *mcgraph* compared to *huge* in support of our general hypothesis. AUC scores ($\overline{x}_{huge} = 0.923$, $\overline{x}_{mcgraph} = 0.938$, $\Delta\overline{x} = -0.016$, CI95% $= [-0.20, -0.012]$, $p < 0.0001$) can be assumed to be biased upwards due to strong negative skewness of the score distribution (see figure 7). As mentioned earlier, AUC is unsuitable for an imbalanced classification set. Scores of PR-AUC ($\overline{x}_{huge} = 0.774$, $\overline{x}_{mcgraph} = 0.823$, $\Delta\overline{x} = -0.049$, CI95% $= [-0.056, -0.041]$, $p < 0.0001$) were considerably lower, reflecting a more conservative evaluation, but the variability of the individual scores was much higher compared to the other metrics especially for *huge* data. While it is better suited for class imbalance (Saito and Rehmsmeier 2015), its valuation scheme is a function of the degree of imbalance (i.e., a graph's sparsity). Consequently, scores are accurate for large class imbalances, but for smaller imbalances the scores should be corrected downwards (Boyd et al. 2012). We did not apply this correction in our study, and it would not change the implications of our main findings, because we concentrated on mean differences between the packages. Still, this should be considered for any follow-up analysis. BCR scores ($\overline{x}_{huge} = 0.795$, $\overline{x}_{mcgraph} = 0.822$, $\Delta\overline{x} = -0.028$, CI95% $= [-0.032, -0.024]$, $p < 0.0001$) showed relatively low variability of individual scores. The same was true for norm-MCC ($\overline{x}_{huge} = 0.775$, $\overline{x}_{mcgraph} = 0.799$, $\Delta\overline{x} = -0.024$, CI95% $= [-0.032, -0.024]$, $p < 0.0001$). The mean scores of the latter were the most conservative. MCC is a total summary score of all outcomes and provides a balanced assessment of the relation of FP and FN. Chicco and Jurman note, that it is mostly the best metric to use, especially in case of class imbalance (Chicco and Jurman 2020).

The results additionally showed that network reconstructs for scale-free networks based on Monte Carlo data were especially well assessed. This is noteworthy, because networks of cells, social relationships or other real-world systems are often characterized by such a structure (Barabási and Oltvai 2004). These networks are not fixed concerning their size, but dynamically grow by preferential attachment (i.e., nodes connect to already high-degree nodes) so that they are characterized by a power-law degree distribution (Barabási 1999; Barabási and Pósfai 2016).

Concerning the relationship of LEH scores and bone growth, we did not find any association. The generated network estimate after stepwise regression showed a cluster graph with two separate components, one component containing all bone related variables and the other one contained all variables related to LEH scores of canines. By and large, this result agreed with the more extensive statistical analysis done by (Mattsson 2021), where SNHA was applied.

Throughout our analysis we used a version of stepwise regression and we have already noted, that this method is problematic. We still used it because (1) in our network reconstruction analysis the true model was known beforehand or in the case of the LEH model, there was at least some model by another method / study we could compare our results with, (2) we also applied a collection of alternative methods in comparison and (3) it seemed, that our implementation based on preselecting covariates by highest correlation, using AIC and R^2 improved empirical results. But this might not help with the fundamental issues, that variables are selected one after another purely based on the underlying data using statistics, which are meant to be applied on prespecified models (Harrell 2001). Thus, despite appearing as a straightforward approach stepwise selection must be used very carefully or should better be replaced with alternative methods (Huberty 1989; Heinze and Dunkler 2017; Smith 2018).

Another possible limitation of our analysis is the use of classification: Classification reduces the degree of information of a signal by binarization, reframing the initial problem as an either-or question. F. E. Harrell notes, that in many circumstances this is not the right way to confront real-world problems and argues for the use of probabilistic model approaches and methods based on bootstrapping instead (Harrell 2001). The last step of our testing framework must not necessarily be based on classification, as we did here, but might well be based on a richer probabilistic approach, where the presence of associations is modeled by probabilities or on bootstrapping to assign empirical confidence intervals for each edge. The important point is that there is a pre-defined structure at hand and suitable randomized data based on it to begin with. Overall, the analysis of synthetic networks can be worthwhile, and our Monte Carlo approach has the advantage of being conceptually and practically simple but extendable. It offers the possibility to use (weighted) un- and directed input graphs for simulation analysis and generates suitable data for it.

Conclusion

Generating synthetic data for graphs and evaluate network reconstructs of methods of interest, can be one step in the process of method verification by researchers. The *mcgraph* R package offers various features to create and plot graph structures, as well as to generate synthetic data based on given graph structures for the purpose of network reconstruction. The simple Monte Carlo algorithm presented in this paper generates simulated data with quality at least as good as the comparable R package *huge* for cluster, random, hub and scale-free network types of various sizes. By adjusting a small set of parameters, like the number of samples generated per node the data can be further optimized. The package is currently submitted to the “The Comprehensive R Archive Network” and should be available soon as an official R package.

List of Abbreviations

Abbreviations	Meaning
ADBOU	Anthropological DataBase Odense University
AIC	Akaikes Information Criterion
AUC	Area Under the Receiver Operating Characteristic Curve
BCR	Balance Classification Rate
CI95%	95% Confidence Interval
FN	False Negative
FP	False Positive
FPR	False Positive Rate
IQR	InterQuartile Range
LEH	Linear Enamel Hypoplasia
MCC	Matthews Correlation Coefficient
norm-MCC	nomalized Matthews Correlation Coefficient
PPV	Positive Predictive Value
PR-AUC	Area Under the Precision Recall Curve
PRC	Precision Recall Curve
ROC	Receiver Operating Characteristic Curve
SNHA	St. Nicolas House Analysis
TN	True Negative
TNR	True Negative Rate or specificity
TP	True Positive
TPR	True Positive Rate, sensitivity or recall

References

Akaike, H. (1974). A new look at the statistical model identification. IEEE Transactions on Automatic Control 19 (6), 716–723. https://doi.org/10.1109/TAC.1974.1100705.

Barabási, A.-L. (1999). Emergence of scaling in random networks. Science 286 (5439), 509–512. https://doi.org/10.1126/science.286.5439.509.

Barabási, A.-L. (2007). Network medicine – from obesity to the "Diseasome". The New England Journal of Medicine 357 (4), 404–407. https://doi.org/10.1056/NEJMe078114.

Barabási, A.-L./Gulbahce, N./Loscalzo, J. (2011). Network medicine: a network-based approach to human disease. Nature Reviews Genetics 12 (1), 56–68. https://doi.org/10.1038/nrg2918.

Barabási, A.-L./Oltvai, Z. N. (2004). Network biology: understanding the cell's functional organization. Nature Reviews Genetics 5 (2), 101–113. https://doi.org/10.1038/nrg1272.

Barabási, A.-L./Pósfai, M. (2016). Network science. Cambridge, Cambridge University Press.

Batushansky, A./Toubiana, D./Fait, A. (2016). Correlation-Based Network Generation, Visualization, and Analysis as a Powerful Tool in Biological Studies: A Case Study in Cancer Cell Metabolism. BioMed Research International 2016, 8313272. https://doi.org/10.1155/2016/8313272.

Berrar, D./Granzow, M./Dubitzky, W. (2007). Fundamentals of data mining in genomics and proteomics. Boston, MA, Springer; Springer US.

Boyd, K./Santos Costa, V./Davis, J./Page, C. D. (2012). Unachievable region in precision-recall space and its effect on empirical evaluation. In: J. Langford/J. Pineau (Eds.). Proceedings of the 29th International Conference on Machine Learning // Proceedings of the Twenty-Ninth International Conference on Machine Learning. Edinburgh, [International Machine Learning Society], 1616–1626.

Breiman, L./Friedman, J. H./Olshen, R. A./Stone, C. J. (1984). Classification and regression trees. Belmont, Calif., Wadsworth.

Büttner, K./Salau, J./Krieter, J. (2016). Adaption of the temporal correlation coefficient calculation for temporal networks (applied to a real-world pig trade network). SpringerPlus 5, 165. https://doi.org/10.1186/s40064-016-1811-7.

Cao, C./Chicco, D./Hoffman, M. M. (2020). The MCC-F1 curve: a performance evaluation technique for binary classification. https://doi.org/10.48550/arXiv.2006.11278.

Chicco, D./Jurman, G. (2020). The advantages of the Matthews correlation coefficient (MCC) over F1 score and accuracy in binary classification evaluation. BMC Genomics 21 (1), 6. https://doi.org/10.1186/s12864-019-6413-7.

Christakis, N. A./Fowler, J. H. (2007). The spread of obesity in a large social network over 32 years. New England Journal of Medicine 357 (4), 370–379. https://doi.org/10.1056/NEJMsa066082.

Copas, J. B./Long, T. (1991). Estimating the residual variance in orthogonal regression with variable selection. The Statistician 40 (1), 51–59. https://doi.org/10.2307/2348223.

Dahl, D. B./Scott, D./Roosen, C./Magnusson, A./Swinton, J. (2000). xtable: Export Tables to LaTeX or HTML. Available online at https://CRAN.R-project.org/package=xtable (accessed 5/31/2022).

Eddelbuettel, D./François, R. (2011). Rcpp: Seamless R and C++ integration. Journal of Statistical Software 40 (8), 1–18. https://doi.org/10.18637/jss.v040.i08.

Eddelbuettel, D./Sanderson, C. (2014). RcppArmadillo: Accelerating R with high-performance C++ linear algebra. Computational Statistics and Data Analysis 71, 1054–1063. https://doi.org/10.1016/j.csda.2013.02.005.

Efron, B./Tibshirani, R. (1986). Bootstrap methods for standard errors, confidence intervals, and other measures of statistical accuracy. Statistical Science 1 (1), 54–75. https://doi.org/10.1214/ss/1177013815.

Frayling, T. M./Timpson, N. J./Weedon, M. N./Zeggini, E./Freathy, R. M./Lindgren, C. M./Perry, J. R. B./Elliott, K. S./Lango, H./Rayner, N. W./Shields, B./Harries, L. W./Barrett, J. C./Ellard, S./Groves, C. J./Knight, B./Patch, A./Ness, A. R./Ebrahim, S./Lawlor, D. A./Ring, S. M./Ben-Shlomo, Y./Jarvelin, M.-R./Sovio, U./Bennett, A. J./Melzer, D./Ferrucci, L./Loos, R. J. F./Barroso, I./Wareham, N. J./Karpe, F./Owen, K. R./Cardon, L. R./Walker, M./Hitman, G. A./Palmer, C. N. A./Doney, A. S. F./Morris, A. D./Smith, G. Davey/Hattersley, A. T./McCarthy, M. I. (2007). A common variant in the FTO gene is associated with body mass index and predisposes to childhood and adult obesity. Science 316 (5826), 889–8894. https://doi.org/10.1126/science.1141634.

Friedman, J./Hastie, T./Tibshirani, R. (2008). Sparse inverse covariance estimation with the graphical lasso. Biostatistics 9 (3), 432–441. https://doi.org/10.1093/biostatistics/kxm045.

Ghazalpour, A./Doss, S./Zhang, B./Wang, S./Plaisier, C./Castellanos, R./Brozell, A./Schadt, E. E./Drake, T. A./Lusis, A. J./Horvath, S. (2006). Integrating genetic and network analysis to characterize genes related to mouse weight. PLOS 2 (8), 1182–1192. https://doi.org/10.1371/journal.pgen.0020130.

Groth, D./Novine, M. (2022). mcgraph. Available online at https://github.com/MasiarNovine/mcgraph (accessed 1/18/2022).

Groth, D./Scheffler, C./Hermanussen, M. (2019). Body height in stunted Indonesian children depends directly on parental education and not via a nutrition mediated pathway – Evidence from tracing association chains by St. Nicolas House Analysis. Anthropologischer Anzeiger 76 (5), 445–451. https://doi.org/10.1127/anthranz/2019/1027.

Hanley, J. A./McNeil, B. J. (1982). The meaning and use of the area under a receiver operating characteristic (ROC) curve. Radiology 143 (1), 29–36. https://doi.org/10.1148/radiology.143.1.7063747.

Harrell, F. E. (2001). Regression modeling strategies – with applications to linear models, logistic regression, and survival analysis. 2nd ed. New York, Springer.

Heinze, G./Dunkler, D. (2017). Five myths about variable selection. Transplant International 30 (1), 6–10. https://doi.org/10.1111/tri.12895.

Heinze, G./Wallisch, C./Dunkler, D. (2018). Variable selection – A review and recommendations for the practicing statistician. Biometrical Journal 60 (3), 431–449. https://doi.org/10.1002/bimj.201700067.

Hermanussen, M./Aßmann, C./Groth, D. (2021). Chain reversion for detecting associations in interacting variables – St. Nicolas house analysis. International journal of environmental research and public health 18 (4), 1741. https://doi.org/10.3390/ijerph18041741.

Huberty, C. J. (1989). Problems with stepwise methods – better alternatives. Advances in Social Science Methodology (1), 43–70.

Jiang, H./Fei, X./Liu, H./Roeder, K./Lafferty, J./Wasserman, L./Li, X./Zhao, T. (2021). High-dimensional undirected graph estimation. Available online at https://cran.r-project.org/web/packages/huge/huge.pdf (accessed 1/18/2022).

Langfelder, P./Horvath, S. (2008). WGCNA: an R package for weighted correlation network analysis. BMC Bioinformatics 9, 559. https://doi.org/10.1186/1471-2105-9-559.

Loscalzo, J./Barabási, A.-L./Silverman, E. (2017). Network medicine: Complex systems in human disease and therapeutics. Cambridge, Harvard University Press.

Matthews, B. W. (1975). Comparison of the predicted and observed secondary structure of T4 phage lysozyme. Biochimica et Biophysica Acta (BBA) – Protein Structure 405 (2), 442–451. https://doi.org/10.1016/0005-2795(75)90109-9.

Mattsson, C. C. (2021). Correlation between childhood episodes of stress and long bone-ratios in samples of medieval skeletons – using linear enamel hypoplasia as proxy. Human Biology and Public Health 3. https://doi.org/10.52905/hbph2021.3.23.

Meinshausen, N./Bühlmann, P. (2006). High-dimensional graphs and variable selection with the Lasso. The Annals of Statistics 34 (3), 1436–1462. https://doi.org/10.1214/009053606000000281.

Meinshausen, N./Bühlmann, P. (2010). Stability selection. Journal of the Royal Statistical Society. Series B, Statistical Methodology 72 (4), 417–473. https://doi.org/10.1111/j.1467-9868.2010.00740.x.

Metropolis, N./Ulam, S. (1949). The Monte Carlo method. Journal of the American Statistical Association 44 (247), 335–341. https://doi.org/10.2307/2280232.

Milner, G. R./Boldsen, J. L. (2012). Transition analysis: a validation study with known-age modern American skeletons. American Journal of Physical Anthropology 148 (1), 98–110. https://doi.org/10.1002/ajpa.22047.

Nicosia, V./Tang, J./Mascolo, C./Musolesi, M./Russo, G./Latora, V. (2013). Graph metrics for temporal networks. In: P. Holme/J. Saramäki (Eds.). Temporal networks. Petter Holme; Jari Saramäki, eds. Heidelberg, Springer, 15–40.

R Core Team (2021). R: a language and environment for statistical computing. R Foundation for Statistical Computing. Available online at https://www.r-project.org/.

Rice, J. J./Tu, Y./Stolovitzky, G. (2005). Reconstructing biological networks using conditional correlation analysis. Bioinformatics 21 (6), 765–773. https://doi.org/10.1093/bioinformatics/bti064.

Saito, T./Rehmsmeier, M. (2015). The precision-recall plot is more informative than the ROC plot when evaluating binary classifiers on imbalanced datasets. PLOS ONE 10 (3), 1–21. https://doi.org/10.1371/journal.pone.0118432.

Sakamoto, Y./Ishiguro, M./Kittagawa, G. (1986). Akaike information criterion statistics. Dordrecht, Reidel.

Sanderson, C./Curtin, R. (2016). Armadillo: a template-based C++ library for linear algebra. Journal of Open Source Software 1 (2), 26. https://doi.org/10.21105/joss.00026.

Sanderson, Conrad/Curtin, Ryan (2018). A user-friendly hybrid sparse matrix class in C++. In: J. H. Davenport/M. Kauers/G. Labahn et al. (Eds.). Mathematical Software – ICMS 2018. 6th International Conference, South Bend, IN, USA, July 24–27, 2018, Proceedings. Cham, Springer International Publishing, 422–430.

Smith, G. (2018). Step away from stepwise. Journal of Big Data 5 (1), 32. https://doi.org/10.1186/s40537-018-0143-6.

Sulaimanov, N./Koeppl, H. (2016). Graph reconstruction using covariance-based methods. EURASIP Journal on Bioinformatics and Systems 19 // 2016 (1), 267–288. https://doi.org/10.1186/s13637-016-0052-y.

Tarp, P. (2017). Skeletal age estimation: a demographic study of the population of Ribe through 1000 years. Ph.D. dissertation. Odense, Syddansk Universitet.

Wasserman, L. (2013). All of statistics: a concise course in statistical inference. A concise course in statistical inference. New York, Springer.

Wasserman, S./Faust, K. (1994). Social network analysis: methods and applications. Cambridge, Cambridge University Press.

Wickham, H. (2016). ggplot2: elegant graphics for data analysis. 2nd ed. Cham, Springer.

Xie, Y. (2021). knitr: A General-purpose package for dynamic report generation in R. Available online at https://yihui.org/knitr/.

Zhang, B./Horvath, S. (2005). A general framework for weighted gene co-expression network analysis. Statistical Applications in Genetics and Molecular Biology 4, 17. https://doi.org/10.2202/1544-6115.1128.

Zhao, T./Liu, H./Roeder, K./Lafferty, J./Wasserman, L. (2012). The huge package for high-dimensional undirected graph estimation in R. Journal of Machine Learning Research 13, 1059–1062.

Appendix

Table 2 List of arguments and guidelines for parameters of the Monte Carlo algorithm. Argument, description with guidelines and default values of the Monte Carlo algorithm implemented in the R package mcgraph (Groth and Novine 2022).

Argument	Description	Default
A	Input graph. This can be a (weighted) directed or undirected graph, given as an adjacency matrix.	-
n	The number of generated data values for each variable. The initial values are drawn from a normal distribution as described before. More values should lead to pronounced correlations and better reconstructs but will increase the runtime and memory allocation.	200
iter	The number of iterations, (i.e., the steps of refinement of the data). In each iteration the values of outgoing neighboring nodes become more and more similar. This argument counteracts *noise* (i.e., more iteration steps should decrease the influence of *noise* and allow for more pronounced correlations but only to an upper bound).	30
val	The given mean value of the normal distribution the random values are drawn from. The default value of 100 is chosen based on practical considerations: *noise*, which is added after each iteration and drawn from a normal distribution with a mean of 0, should only be a small fraction of the data values.	100
sd	The given value for the standard deviation of the normal distribution the random values are drawn from. The default value of 2 is chosen to allow for a sufficiently large spread of the initial values.	2
prop	The proportion, which determines how the values of the respective source and target node are weighted when calculating the updated value of the target in each iteration. Larger values increase the weighting of the source and decrease the weighting of the target for the calculation of the weighted mean.	0.05
noise	The level of random noise, which is added to the data values in each iteration step. It indicates the value for the standard deviation of a normal distribution with mean 0 from which values are drawn randomly. The influence of *noise* is dependent on *val* (i.e., higher values for *noise* will lead to less pronounced correlations between variables). We use a normal distribution with mean 0 to let *noise* only be small fraction of *val*. This can be counterbalanced by increasing the value for *iter*.	1
init	An optional argument to prespecify an alternative set of starting data.	NULL